

A Fluorinated Ligand Enables Room-Temperature and Regioselective Pd-Catalyzed Fluorination of Aryl Triflates and Bromides

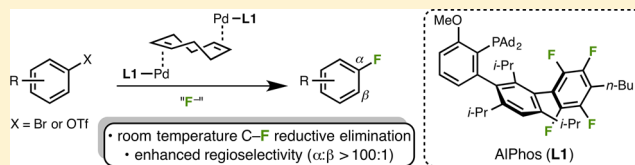
Aaron C. Sather,[†] Hong Geun Lee,[†] Valentina Y. De La Rosa,[†] Yang Yang,^{†,‡} Peter Müller,[†] and Stephen L. Buchwald^{*,†}

[†]Department of Chemistry, Massachusetts Institute of Technology, Cambridge, Massachusetts 02139, United States

[‡]Department of Chemistry, University of Pittsburgh, Pittsburgh, Pennsylvania 15260, United States

S Supporting Information

ABSTRACT: A new biaryl monophosphine ligand (AlPhos, L1) allows for the room-temperature Pd-catalyzed fluorination of a variety of activated (hetero)aryl triflates. Furthermore, aryl triflates and bromides that are prone to give mixtures of regioisomeric aryl fluorides with Pd-catalysis can now be converted to the desired aryl fluorides with high regioselectivity. Analysis of the solid-state structures of several Pd(II) complexes, as well as density functional theory (DFT) calculations, shed light on the origin of the enhanced reactivity observed with L1.



INTRODUCTION

The preparation of fluorine-containing aromatic compounds (ArF) has been a long-standing challenge in organic synthesis.¹ While these compounds are highly prized in the pharmaceutical² and agrochemical industries,³ methods to access aryl fluorides selectively, under mild and general reaction conditions, remain elusive. Since the advent of the Balz–Schiemann⁴ reaction and the Halex⁵ process, significant advances have been made toward this end,⁶ especially with regard to transition metal-catalyzed methods.⁷ In analogy to the practicality, simplicity, and generality of Pd(0)/Pd(II)-catalyzed aryl carbon–heteroatom bond-forming processes, the coupling of aryl (pseudo)halides with simple metal fluoride salts (“F[−]”) (Figure 1a) would be ideal. However, several challenges associated with developing such a process have been revealed both experimentally⁸ and theoretically.⁹ Among these difficulties are the formation of stable [LPd(II)F]₂ dimers and

competitive P–F and P–C bond formation, which suggests a high barrier for C–F reductive elimination (Figure 1a). To circumvent the difficult reductive elimination from Pd(II) complexes, electrophilic fluorine sources (“F⁺”) have been employed to oxidize the metal center to Pd(III) or Pd(IV) intermediates from which reductive elimination is more facile.¹⁰

The desired C–F reductive elimination from [LPdAr(F)] is unique to biaryl monophosphine-ligated complexes, and has been observed stoichiometrically,¹¹ albeit at high temperatures and with substrates that contain activated¹² aryl groups. Subsequently, it was discovered that incorporating a substituent at the C3′ position of the biaryl monophosphine ligand, for example, as in HGPhos ((L2), Figure 1b), gives rise to a more active catalyst system.¹³

While these discoveries have shown that Pd(II)-catalyzed fluorination is indeed viable, several problems remain. Most importantly, the generation of regioisomeric byproducts¹⁴ (presumably through a Pd–benzyne intermediate) lowers the yield of the desired product and renders purification difficult or even impossible. Additionally, the use of elevated reaction temperatures is required to achieve full conversion of the starting materials. To address these issues, which we ascribe to the difficult C–F reductive elimination from Pd(II) complexes, we sought to design a ligand to improve this elementary step as well as the overall efficiency of the catalytic transformation. As shown in Figure 1b, biaryl monophosphine ligands coordinate to the Pd(II) metal center in a bidentate fashion, making contacts through both the phosphine and the C1′ carbon of the adjacent aromatic ring.¹⁵ Because reductive elimination from Pd(II) complexes is typically favored from a three-coordinate intermediate,¹⁶ we hypothesized that modification at C3′ with

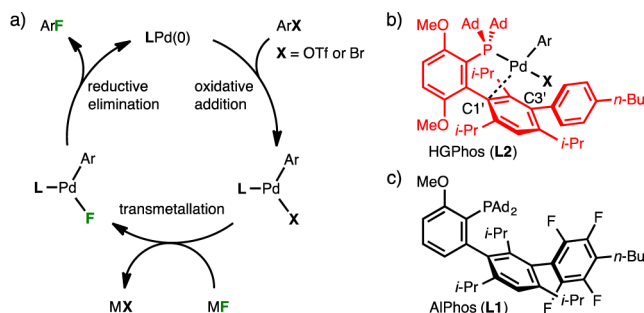


Figure 1. (a) The proposed catalytic cycle for Pd-catalyzed fluorination. (b) A Pd(II) complex with L2 highlighted in red. The interaction between ligand-bound Pd(II) and C1′ is shown by a dashed line. (c) Biaryl monophosphine ligand (Alphos, L1).

Received: September 2, 2015

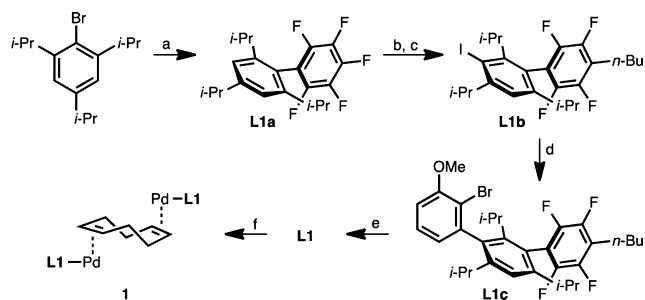
Published: September 28, 2015

an electron-withdrawing group would diminish the donation of electron density from C1' to the Pd(II) metal center, providing an intermediate with more three-coordinate character and thereby generating a more active catalyst.

RESULTS AND DISCUSSION

To test our hypothesis, we designed and synthesized a ligand that was less electron-rich than the previously reported L2. This

Scheme 1. Synthesis of L1 and Pd(0) Precatalyst 1^a



^aReagents and conditions: (a) THF, $-78\text{ }^{\circ}\text{C}$, *n*-BuLi, 1 h; added to C_6F_6 in THF, $0\text{ }^{\circ}\text{C}$ to rt, 2 h, 87%. (b) THF, $-78\text{ }^{\circ}\text{C}$, *n*-BuLi, 30 min, 99%. (c) AcOH, EtOAc, H_2SO_4 , *N*-iodosuccinimide, $50\text{ }^{\circ}\text{C}$, 17 h, 80%. (d) THF, $-78\text{ }^{\circ}\text{C}$, *t*-BuLi, 1 h; added to 3-fluoroanisole and *n*-BuLi in THF, -78 to $-25\text{ }^{\circ}\text{C}$, 44%. (e) THF, $-78\text{ }^{\circ}\text{C}$, *t*-BuLi, 1 h; CuCl $-78\text{ }^{\circ}\text{C}$ to rt; Ad_2PCL , toluene, $140\text{ }^{\circ}\text{C}$, 18 h, 82%. (f) $[\text{COD-Pd}(\text{CH}_2\text{TMS})_2]$, pentane, rt, 48 h, 78%.

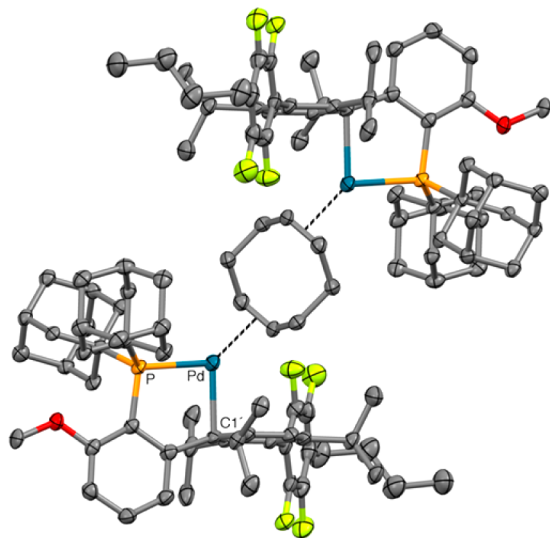
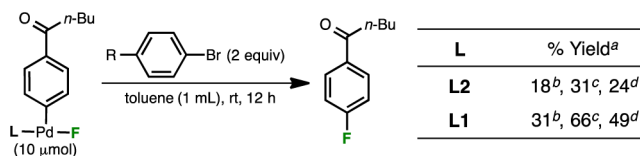


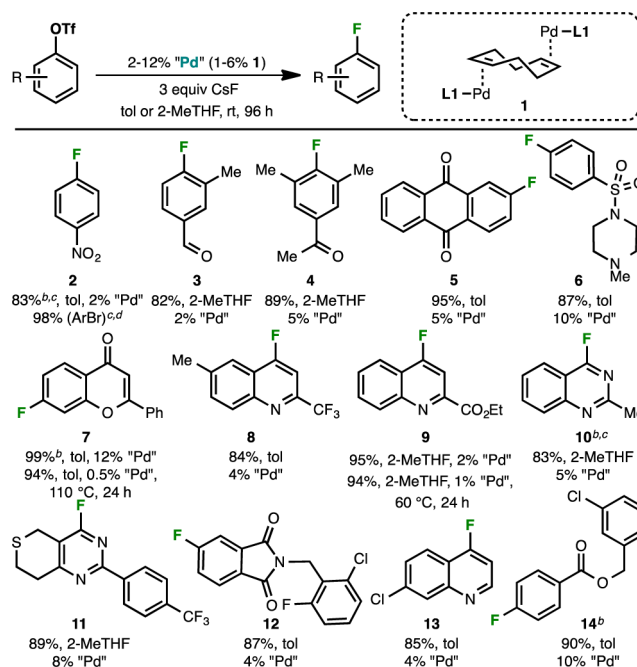
Figure 2. Crystal structure of $[(\text{L1Pd})_2\text{-COD}]$ (1). Thermal ellipsoids are shown at 50% probability; hydrogen atoms and residual benzene molecules are omitted for clarity.

Scheme 2. Stoichiometric C–F Reductive Elimination from Pd(II) Complexes at Room Temperature^a



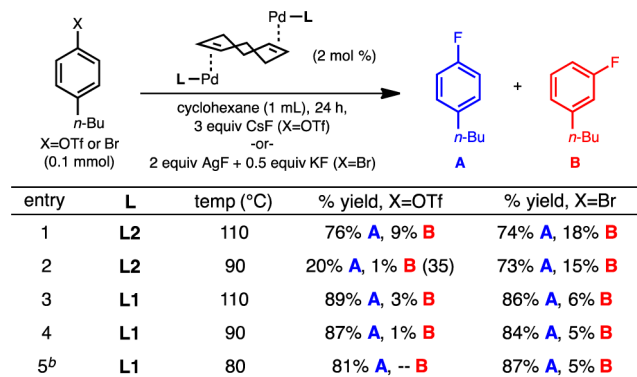
^aYields determined by ^{19}F NMR. ^bNo ArBr added. ^cArBr ($\text{R} = \text{C}(\text{O})n\text{-Bu}$). ^dArBr ($\text{R} = n\text{-Bu}$).

Table 1. Room-Temperature Fluorination of Aryl Triflates^a



^aIsolated yields are reported as an average of two runs. Reaction conditions unless otherwise noted: Aryl triflate (1 mmol), CsF (3 mmol), tol or 2-MeTHF (10 mL). ^b0.50 mmol scale. ^c ^{19}F NMR yield. ^dAryl bromide (0.5 mmol), KF (0.25 mmol), AgF (1.0 mmol), tol (5 mL). tol = toluene, 2-MeTHF = 2-methyl tetrahydrofuran.

Table 2. Temperature Dependence on Regioisomer Formation^{a,b}



^aYields were determined by ^{19}F NMR. Numbers in parentheses indicate % conversion of the starting material. ^bThe reaction time was 48 h.

was accomplished by removing the methoxy group adjacent to the dialkylphosphino group on the "upper" aromatic ring and replacing the hydrogen atoms of the pendant 4-(*n*-Bu)Ph group at C3' with fluorines¹⁷ (Figure 1c). The synthesis of L1 is described in Scheme 1. Lithium–halogen exchange of 2,4,6-triisopropylbromobenzene with *n*-BuLi followed by nucleophilic addition into hexafluorobenzene provides perfluoro biaryl L1a. To improve solubility of the final ligand and prevent subsequent nucleophilic additions into the activated perfluoro aromatic, *n*-BuLi was added at $-78\text{ }^{\circ}\text{C}$ to give the alkylated product via $\text{S}_{\text{N}}\text{Ar}$, which was then halogenated using *N*-iodosuccinimide and H_2SO_4 to yield L1b. Terphenyl L1c was prepared by nucleophilic addition of L1b into a benzyne

Table 3. Regioselective Fluorination^{a,b,c}

X = OTf or Br			
 15 94% (X=OTf), 28 h <i>p.m</i> = >300:1 96% (X=Br) ^d , 24 h 1% "Pd", 90 °C <i>p.m</i> = 125:1	 16 94% (X=OTf), 24 h 2% "Pd", 120 °C $\alpha\beta$ = 199:1	 17^c 98% (X=OTf), 24 h 2% "Pd", 90 °C <i>m.p</i> = 120:1	 18^a 96% (X=OTf), 24 h 2% "Pd", 90 °C
 19 81% (X=OTf), 28 h 2% "Pd", 90 °C $\alpha\beta$ = 250:1	 20 95% (X=OTf) ^e , 24 h 96% (X=Br) ^b , 24 h <i>m.p</i> = 255:1 2% "Pd", 110 °C	 21^{c,d,e} 77% (X=OTf), 17 h 91% ^b (X=Br), 17 h 2% "Pd", 100 °C	 22^{c,d} 44% (X=OTf), 24 h 10% "Pd", 90 °C <i>p.m</i> = 21:1 90% ^b (X=Br), 24 h 4% "Pd", 110 °C <i>p.m</i> = 2.2:1
 23^a 96% (X=OTf), 24 h 2% "Pd", 90 °C	 24^c 87% (X=OTf), 48 h, 10% "Pd", 70 °C <i>p.m</i> = 150:1	 25 92% (X=OTf), 24 h 2% "Pd", 90 °C <i>p.m</i> = 102:1	

^aIsolated yields are reported as an average of two runs. Reaction conditions unless otherwise noted: Aryl triflate (1 mmol), CsF (3 mmol), cy (10 mL). ^bAryl bromide (1 mmol), KF (0.5 mmol), AgF (2.0 mmol), cy (10 mL). ^c0.5 mmol scale. ^d¹⁹F NMR yield. ^eNo regioisomer detected by ¹⁹F NMR. cy = cyclohexane.

intermediate, generated from 3-fluoroanisole, followed by quenching the resulting aryl anion with bromine at -30 °C. Treatment of **L1c** with *t*-BuLi at -78 °C followed by the addition of CuCl and Ad₂PdCl and then heating to 140 °C overnight furnished **L1** in 82% yield (25% yield over five steps). The synthesis was amenable to scale up as more than 10 g of **L1** was prepared in a single batch.

The highly active Pd(0) precatalyst [(L1Pd)₂·COD] (**1**) was prepared in 78% yield by treating **L1** with an equivalent of [COD·Pd(CH₂TMS)₂] in pentane, which could be easily isolated and stored under an inert atmosphere (Scheme 1).^{18,19} Because of the electron-rich nature and high reactivity of biaryl monophosphine-ligated Pd(0) complexes, there exist only a few structurally characterized examples.²⁰ We have previously described several Pd(0) precatalysts, of which indirect evidence was obtained suggesting an empirical formula of [(LPd)_n·COD] (*n* = 1–2); however, the insolubility of these complexes precluded structural characterization by single-crystal X-ray diffraction.^{13c,18} Single crystals of **1** suitable for X-ray diffraction were obtained providing the first structural evidence for this class of precatalyst (Figure 2). Complex **1** crystallizes in the triclinic centrosymmetric space group P1̄ with half a molecule of **1** and three molecules of benzene per asymmetric unit. The second half of **1** is generated by the crystallographic inversion center. The full molecule is a binuclear complex in which each Pd atom is chelated by one **L1** ligand. Located between the two palladium centers is a cyclooctadiene molecule (COD), which coordinates through its two double bonds to the metal atoms in a side-on fashion that can be described as η₂. This results in a distorted trigonal planar coordination environment for the palladium atoms with the following angles: P–Pd–C1', 88°; P–Pd–COD, 135°; and C1'–Pd–COD, 137°.

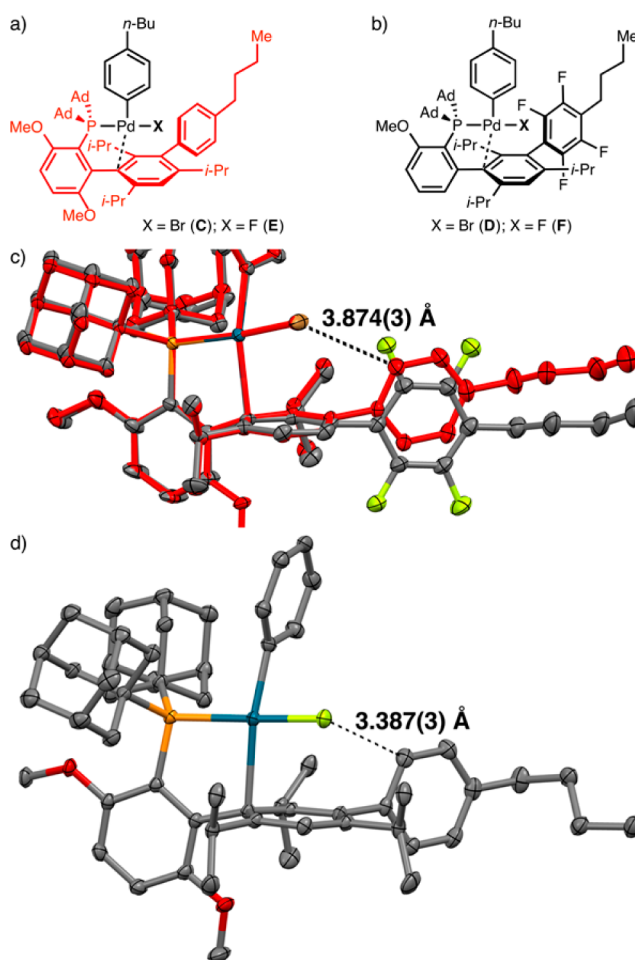


Figure 3. (a) Schematic of [L2Pd(Ar)X] complexes C and E where L2 is highlighted in red. (b) Schematic of [L1Pd(Ar)X] complexes D and F. (c) Crystal structure overlay of C and D. C is shown in red. Hydrogen atoms and an isopropyl group are omitted for clarity. (d) Crystal structure of E highlighting the intramolecular CH...F contact. Hydrogen atoms and the *n*-butyl group on the Pd-bound aryl omitted for clarity. Thermal ellipsoids are shown at 50% probability.

The reactivity of **L1** and **L2** was compared by preparing analogous [LPdAr(F)] complexes and examining the formation of the ArF resulting from the stoichiometric C–F reductive elimination from the Pd(II) intermediates at room temperature (Scheme 2). These reactions were performed in the presence and absence of added aryl bromide, which serves as a trapping agent for the resulting Pd(0) that is formed after reductive elimination.^{21,13a} After a period of 12 h, the **L1**-supported complex provides approximately twice the amount of the desired product than that bearing **L2**. Both **L1**- and **L2**-ligated complexes provided the ArF product and are the first examples of room-temperature C–F reductive elimination from isolated [LPd(Ar)F] complexes.

The enhanced reactivity in the stoichiometric process exhibited by the **L1**-supported Pd(Ar)F complex was successfully extended to the catalytic reaction. By using **1**, a variety of activated (hetero)aromatic triflates (Table 1) were transformed to the fluoride derivatives at room temperature.²² A range of functional groups were tolerated in this transformation, including nitro (**2**), formyl (**3**), methyl ketone (**4**), redox active anthraquinone (**5**), and sulfonamide/tertiary amine (**6**). Heteroaryl triflates were also competent substrates

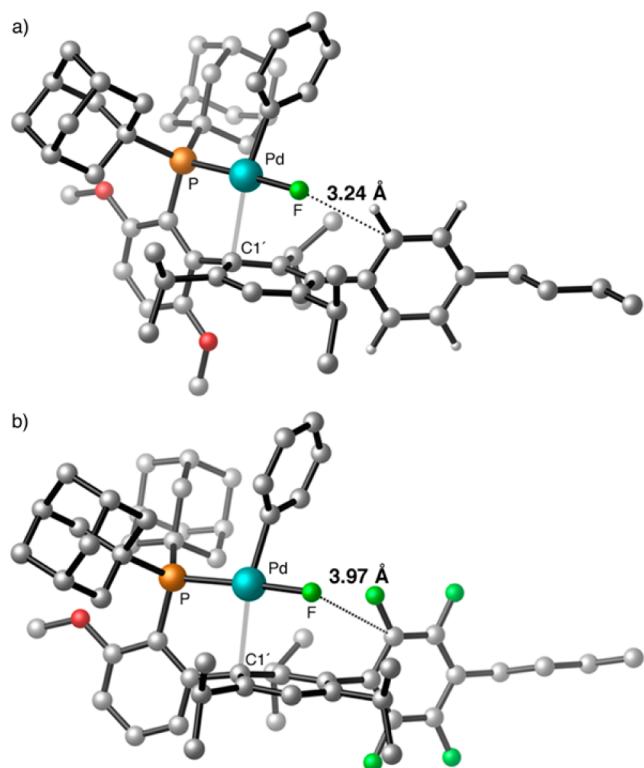


Figure 4. Computed ground-state structures of complexes E' and F'. Geometries were optimized at the B3LYP/6-31G(d)-SDD(Pd) level of theory. Hydrogen atoms are omitted for clarity. (a) The CH...F interaction of complex E' is 3.24 Å, measured from C to F. (b) Complex F' showing the lack of an intermolecular stabilizing interaction.

as flavone **7**, quinolines **8** and **9**, and quinazoline **10** derivatives were prepared in high yields. Notably, XAV939,²³ a tankyrase inhibitor and potential cancer therapeutic, could be fluorinated to give **11**, demonstrating the applicability of this method to fluorinate medically relevant compounds. Additionally, aryl triflates can be selectively transformed in the presence of aryl chlorides, leaving a reactive handle for downstream modifications (**12**–**14**). While the long reaction times at room temperature speak to the stability of the catalyst, the transformation can be completed in 24 h by increasing the temperature even while lowering the catalyst loading (Table 1, **7** and **9**).

With our previously described catalyst systems,^{11,13,14} mixtures of regioisomeric aryl fluorides are sometimes formed during the Pd-catalyzed nucleophilic fluorination reaction.¹⁴ In general, substrates with *para* electron-donating groups or *meta* substitution are plagued by this undesired reaction pathway. Previously, by using cyclohexane as the solvent, the amount of regioisomer formation could be reduced. In some instances, however, the quantity of undesired regioisomer formed was still significant.

To probe the effectiveness of catalysts derived from **1** to further suppress the formation of regioisomeric byproducts, we examined 4-(*n*-Bu)PhOTf (X = OTf) and 4-(*n*-Bu)PhBr (X = Br) as model substrates (Table 2). With either aryl electrophile, the L2-supported precatalyst provides substantial amounts of undesired isomer **B** (entry 1). The enhanced reactivity of **1**, however, allows for the use of lower reaction temperatures than were previously possible (entry 2, X = OTf), revealing a

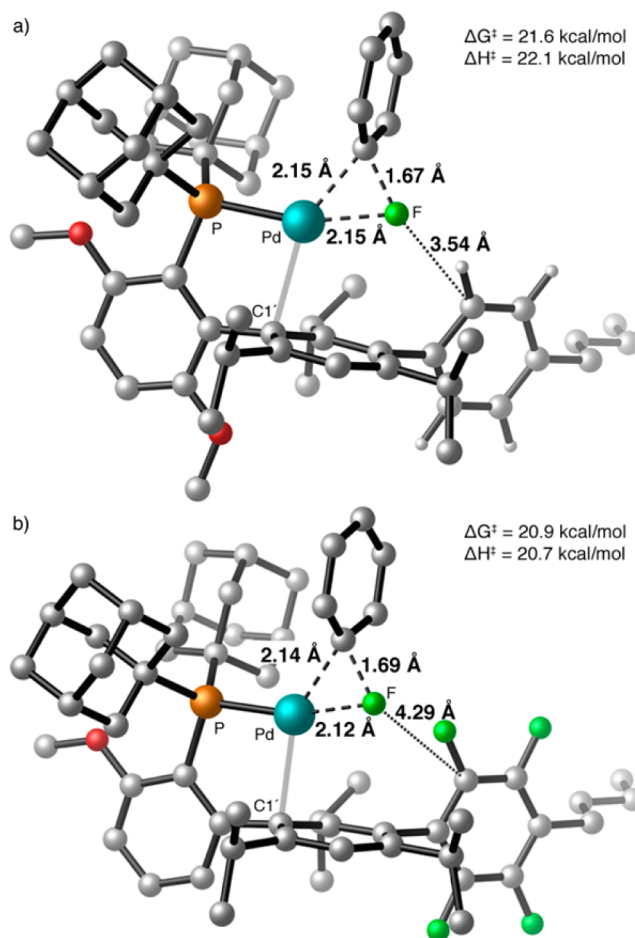


Figure 5. Energies were computed at the M06/6-311+G(d,p)-SDD(Pd)/SMD(toluene) level of theory with geometries optimized at the B3LYP/6-31G(d)-SDD(Pd) level. Hydrogen atoms are omitted for clarity. (a) Transition state minimization of complex E'. (b) Transition state minimization of complex F'.

temperature dependence on the formation of **B** (entries 3–5, X = OTf). The same temperature dependence is not observed for aryl bromides, although using **1** diminishes the amount of **B** formed. Currently, we have no explanation for this dichotomy.

The success of **1** in suppressing the formation of **B** with 4-(*n*-Bu)phenyl triflate or bromide prompted us to study the reaction of a number of substrates that are prone to give regioisomeric mixtures of ArF products. As shown in Table 3, a variety of aryl triflates and bromides converted to the corresponding aryl fluorides in high yield with >100:1 selectivity for the desired regioisomer (**15**–**21**, **23**–**25**). Previously, substrates with strongly electron-donating groups in the *para* position, such as –OMe, have been the most challenging substrates for this methodology. For example, 4-methoxyphenyl triflate¹⁵ and 4-bromoanisole^{13c} have previously been shown to form the undesired *meta* isomer as the major product. Using **1**, the observed selectivity is reversed and the desired product dominates (**22**). Several fluorinated analogues of biologically active compounds were also prepared to give (±)-naproxen **23**, diethylstilbestrol **24**, and tyrosine **25** derivatives with exceptional selectivity. No loss in stereochemical integrity was observed with **25** under the reaction conditions, and reduction (ArH) was only observed for **16** (0.75%), **19** (0.64%), and **22** (0.52%) (see the Supporting Information).²⁴

To gain further insight into the enhanced reactivity of **1**, we prepared the [LPd(Ar)Br] complexes, from the reaction of 4-(*n*-Bu)PhBr and CODPd(CH₂TMS)₂ using **L1** and **L2** as supporting ligands (Figure 3) (see the Supporting Information). The respective complexes were characterized in the solid state using single-crystal X-ray diffraction. The initial hypothesis from which the design of **L1** derived predicts that significant lengthening of the C1'–Pd bond would be observed with the more electron-deficient supporting ligand (**L1**). In fact, only a slight increase in this bond length in **D** was apparent, as compared to that seen with **C** (see the Supporting Information).

By overlaying the crystal structures of **C** and **D**, a more subtle difference was, however, revealed (Figure 3c). With **C**, the pendant 4-(*n*-Bu)Ph group of the ligand is shifted toward the Pd-bound bromide to form an aromatic CH^{δ+}⋯Br contact of 3.874(3) Å (measured from C to Br), which is in agreement with typical aromatic CH⋯Br interaction distances found in the solid state (3.7–4.2 Å; measured from C to Br).²⁵ The perfluorinated aryl group of **D** lacks the required hydrogen atom to achieve the same attractive interaction, giving a C⋯Br distance of 4.370(2) Å. The analogous [LPd(Ar)F] complexes were synthesized (**E** and **F**), and single-crystal X-ray analysis of **E** shows that this behavior is conserved, with **E** exhibiting an aromatic CH⋯F interaction distance of 3.387(3) Å (measured from C to F) (Figure 3d). Typical aromatic CH⋯F interaction distances found in the solid state range from 3.3 to 3.7 Å (measured from C to F).²⁵ Unfortunately, all attempts to obtain single crystals of **F** suitable for X-ray diffraction yielded decomposition and/or pseudocrystalline material.

Short CH⋯F contacts are frequently observed in structurally characterized Pd–F complexes. They serve to stabilize the Pd–F bond by alleviating electronic repulsions between the lone pairs on the fluoride atom and the filled d-orbitals of Pd.⁸ As shown in the solid state, **E** achieves this Pd–F bond stabilization intramolecularly while **F** cannot. The lack of an intramolecular CH⋯F interaction in **F** results in ground-state destabilization relative to **E**, which may account for the observed enhancement in reactivity.

Density functional theory (DFT) calculations were carried out to compare complexes **E** and **F** and gain further insight into the stabilizing CH⋯F interaction that was observed in the solid-state structure of **E**. To reduce conformational complexity, the Pd-bound 4-(*n*-Bu)Ph of complexes **E** and **F** was replaced with a phenyl group in our computational study, giving complexes **E'** and **F'**, respectively. The calculated ground-state structure of **E'** is in good agreement with the crystallographic data of **E**, exhibiting an attractive CH⋯F contact (3.24 Å, measured from C to F) (Figure 4a). Furthermore, NPA (natural population analysis) charge calculations of complex **E'** showed that the Pd-bound fluorine atom bears a partial negative charge of –0.700 and the hydrogen atom at the 2 position of the pendant 4-(*n*-Bu)Ph group carries a partial positive charge of +0.251. Taken together, these analyses clearly indicate the presence of an intramolecular stabilizing interaction. As anticipated, this interaction is absent in complex **F'**, which lacks the necessary hydrogen atom required for this attractive interaction (Figure 4b). In addition, NPA charge analysis of complex **F'** reveals that both the Pd-bound fluorine atom and the fluorine atom at the 2 position of the pendant 4-(*n*-Bu)Ph group carry a partial negative charge (–0.690 and –0.318, respectively), further demonstrating the lack of an attractive interaction in complex **F'**.

Additionally, we performed DFT calculations of the C–F bond-forming reductive elimination step for complexes **E'** and **F'** (Figure 5). This process involves a three-membered transition state where the C–F bond is being formed while the Pd–F and the Pd–C bonds are being broken in a concerted fashion. The calculations showed that the C–F reductive elimination of complex **F'** (Figure 5b) has an activation barrier (ΔG^\ddagger) 0.7 kcal/mol lower than that of complex **E'** (Figure 5a), which is in agreement with the experimentally observed enhanced reactivity of the **L1**-based catalyst.

CONCLUSION

A new ligand (**L1**) that allows for room-temperature C–F reductive elimination from [LPd(Ar)F] has been developed. The enhanced reactivity was exploited to provide aryl fluorides from aryl triflates and bromides with greater than 100:1 selectivity for the desired regioisomer. Crystallographic analysis of several Pd complexes revealed that **L2** provides a stabilizing intramolecular aromatic CH⋯F interaction, which is not accessible with **L1**, giving rise to a more active catalyst system. Finally, DFT calculations were performed comparing complexes **E'** and **F'** corroborating the observations made in the solid state. This study provides insights into ligand structure, which should aid in the discovery and design of more effective catalysts for C–F bond formation.

ASSOCIATED CONTENT

Supporting Information

The Supporting Information is available free of charge on the ACS Publications website at DOI: 10.1021/jacs.5b09308.

Additional procedural, crystallographic, and spectral data (PDF)

X-ray data for six complexes (CIF)

AUTHOR INFORMATION

Corresponding Author

*sbuchwal@mit.edu

Notes

The authors declare the following competing financial interest(s): MIT has obtained patents for the ligands/precatalysts that are described in this Article from which S.L.B. and former/current co-workers receive royalty payments.

ACKNOWLEDGMENTS

This work is dedicated to the grandfather of A.C.S. (Albert B. Sather; AlPhos, **L1**). We thank Drs. Yiming Wang, Michael Pirnot, and John Nguyen for assistance with the preparation of the manuscript. We thank the National Institutes of Health (NIH) for financial support of this research (R01GM46059). A.C.S. thanks the NIH for a postdoctoral fellowship (1F32GM108092-01A1). The content is solely the responsibility of the authors and does not necessarily represent the official views of the NIH. V.Y.D.L.R. thanks the MIT UROP program. We thank Prof. Peng Liu (University of Pittsburgh) for help with computational studies. Calculations were performed at the Center for Simulation and Modeling at the University of Pittsburgh. The X-ray diffractometer was purchased with the help of funding from the National Science Foundation (CHE 0946721).

REFERENCES

- (1) (a) Campbell, M. G.; Ritter, T. *Chem. Rev.* **2015**, *115*, 612. (b) Purser, S.; Moore, P. R.; Swallow, S.; Gouverneur, V. *Chem. Soc. Rev.* **2008**, *37*, 320. (c) Neumann, C. N.; Ritter, T. *Angew. Chem., Int. Ed.* **2015**, *54*, 3216.
- (2) (a) Kirk, K. L. *Org. Process Res. Dev.* **2008**, *12*, 305. (b) Müller, K.; Faeh, C.; Diederich, F. *Science* **2007**, *317*, 1881. (c) Smart, B. E. *J. Fluorine Chem.* **2001**, *109*, 3. (d) Kirsch, P. *Modern Fluoroorganic Chemistry*; Wiley-VCH Verlag GmbH & Co. KGaA: New York, 2013; p 299.
- (3) (a) Jeschke, P. *ChemBioChem* **2004**, *5*, 570. (b) Fujiwara, T.; O'Hagan, D. *J. Fluorine Chem.* **2014**, *167*, 16.
- (4) (a) Balz, G.; Schiemann, G. *Ber. Dtsch. Chem. Ges. B* **1927**, *60*, 1186. (b) Kirk, K. L.; Cohen, L. A. *J. Am. Chem. Soc.* **1973**, *95*, 4619. (c) Cresswell, A. J.; Davies, S. G.; Roberts, P. M.; Thomson, J. E. *Chem. Rev.* **2015**, *115*, 566.
- (5) Finger, G. C.; Kruse, C. W. *J. Am. Chem. Soc.* **1956**, *78*, 6034.
- (6) (a) Fujimoto, T.; Becker, F.; Ritter, T. *Org. Process Res. Dev.* **2014**, *18*, 1041. (b) Sun, H.; DiMagno, S. G. *Angew. Chem., Int. Ed.* **2006**, *45*, 2720. (c) Allen, L. J.; Muhuhji, J. M.; Bland, D. C.; Merzel, R.; Sanford, M. S. *J. Org. Chem.* **2014**, *79*, 5827. (d) Anbarasan, P.; Neumann, H.; Beller, M. *Angew. Chem., Int. Ed.* **2010**, *49*, 2219.
- (7) (a) Tang, P.; Furuya, T.; Ritter, T. *J. Am. Chem. Soc.* **2010**, *132*, 12150. (b) Furuya, T.; Kaiser, H. M.; Ritter, T. *Angew. Chem., Int. Ed.* **2008**, *47*, 5993. (c) Hollingworth, C.; Gouverneur, V. *Chem. Commun.* **2012**, *48*, 2929. (d) Fier, P. S.; Hartwig, J. F. *J. Am. Chem. Soc.* **2012**, *134*, 10795. (e) Ichiishi, N.; Brooks, A. F.; Topczewski, J. J.; Rodnick, M. E.; Sanford, M. S.; Scott, P. J. H. *Org. Lett.* **2014**, *16*, 3224. (f) Casitas, A.; Canta, M.; Solà, M.; Costas, M.; Ribas, X. *J. Am. Chem. Soc.* **2011**, *133*, 19386. (g) Mu, X.; Zhang, H.; Chen, P.; Liu, G. *Chem. Sci.* **2014**, *5*, 275. (h) Truong, T.; Klimovica, K.; Daugulis, O. *J. Am. Chem. Soc.* **2013**, *135*, 9342. (i) Ye, Y.; Schimler, S. D.; Hanley, P. S.; Sanford, M. S. *J. Am. Chem. Soc.* **2013**, *135*, 16292. (j) Wannberg, J.; Wallinder, C.; Ünüsoy, M.; Sköld, C.; Larhed, M. *J. Org. Chem.* **2013**, *78*, 4184. (k) Noël, T.; Maimone, T. J.; Buchwald, S. L. *Angew. Chem., Int. Ed.* **2011**, *50*, 8900.
- (8) (a) Grushin, V. V. *Acc. Chem. Res.* **2010**, *43*, 160. (b) Grushin, V. V.; Marshall, W. J. *Organometallics* **2007**, *26*, 4997. (c) Grushin, V. V. *Chem. - Eur. J.* **2002**, *8*, 1006.
- (9) Yandulov, D. V.; Tran, N. T. *J. Am. Chem. Soc.* **2007**, *129*, 1342.
- (10) (a) Wang, X.; Mei, T.-S.; Yu, J.-Q. *J. Am. Chem. Soc.* **2009**, *131*, 7520. (b) Mazzotti, A. R.; Campbell, M. G.; Tang, P.; Murphy, J. M.; Ritter, T. *J. Am. Chem. Soc.* **2013**, *135*, 14012. (c) Hull, K. L.; Anani, W. Q.; Sanford, M. S. *J. Am. Chem. Soc.* **2006**, *128*, 7134. (d) Chan, K. S. L.; Wasa, M.; Wang, X.; Yu, J.-Q. *Angew. Chem., Int. Ed.* **2011**, *50*, 9081. (e) Pérez-Temprano, M. H.; Racowski, J. M.; Kampf, J. W.; Sanford, M. S. *J. Am. Chem. Soc.* **2014**, *136*, 4097. (f) Ball, N. D.; Sanford, M. S. *J. Am. Chem. Soc.* **2009**, *131*, 3796. (g) Furuya, T.; Benitez, D.; Tkatchouk, E.; Strom, A. E.; Tang, P.; Goddard, W. A.; Ritter, T. *J. Am. Chem. Soc.* **2010**, *132*, 3793. (h) Ding, Q.; Ye, C.; Pu, S.; Cao, B. *Tetrahedron* **2014**, *70*, 409. (i) Lou, S.-J.; Xu, D.-Q.; Xia, A.-B.; Wang, Y.-F.; Liu, Y.-K.; Du, X.-H.; Xu, Z.-Y. *Chem. Commun.* **2013**, *49*, 6218.
- (11) Watson, D. A.; Su, M.; Teverovskiy, G.; Zhang, Y.; García-Fortanet, J.; Kinzel, T.; Buchwald, S. L. *Science* **2009**, *325*, 1661.
- (12) Roy, A. H.; Hartwig, J. F. *J. Am. Chem. Soc.* **2001**, *123*, 1232.
- (13) (a) Maimone, T. J.; Milner, P. J.; Kinzel, T.; Zhang, Y.; Takase, M. K.; Buchwald, S. L. *J. Am. Chem. Soc.* **2011**, *133*, 18106. (b) Milner, P. J.; Maimone, T. J.; Su, M.; Chen, J.; Müller, P.; Buchwald, S. L. *J. Am. Chem. Soc.* **2012**, *134*, 19922. (c) Lee, H. G.; Milner, P. J.; Buchwald, S. L. *J. Am. Chem. Soc.* **2014**, *136*, 3792.
- (14) Milner, P. J.; Kinzel, T.; Zhang, Y.; Buchwald, S. L. *J. Am. Chem. Soc.* **2014**, *136*, 15757.
- (15) Barder, T. E.; Biscoe, M. R.; Buchwald, S. L. *Organometallics* **2007**, *26*, 2183.
- (16) (a) Hoffmann, R. In *IUPAC. Frontiers of Chemistry*; Laidler, K. J., Ed.; Pergamon Press: Oxford, 1982; p 247. (b) Tatsumi, K.; Hoffmann, R.; Yamamoto, A.; Stille, J. K. *Bull. Chem. Soc. Jpn.* **1981**, *54*, 1857.
- (17) (a) Yagupol'skii, L. M.; Ya Il'chenko, A.; Kondratenko, N. V. *Russ. Chem. Rev.* **1974**, *43*, 32. (b) Hansch, C.; Leo, A.; Taft, R. W. *Chem. Rev.* **1991**, *91*, 165.
- (18) (a) Lee, H. G.; Milner, P. J.; Colvin, M. T.; Andreas, L.; Buchwald, S. L. *Inorg. Chim. Acta* **2014**, *422*, 188. (b) Lee, H. G.; Milner, P. J.; Buchwald, S. L. *Org. Lett.* **2013**, *15*, 5602.
- (19) The unreacted ligand could be reisolated from the reaction mixture, allowing **1** to be prepared on the gram scale without losing appreciable amounts of **L1** (see the [Supporting Information](#)).
- (20) (a) Tschan, M. J. L.; García-Suárez, E. J.; Freixa, Z.; Launay, H.; Hagen, H.; Benet-Buchholz, J.; van Leeuwen, P. W. N. M. *J. Am. Chem. Soc.* **2010**, *132*, 6463. (b) Barder, T. E.; Walker, S. D.; Martinelli, J. R.; Buchwald, S. L. *J. Am. Chem. Soc.* **2005**, *127*, 4685. (c) Walker, S. D.; Barder, T. E.; Martinelli, J. R.; Buchwald, S. L. *Angew. Chem., Int. Ed.* **2004**, *43*, 1871. (d) Andreu, M. G.; Zapf, A.; Beller, M. *Chem. Commun.* **2000**, 2475.
- (21) Baranano, D.; Hartwig, J. F. *J. Am. Chem. Soc.* **1995**, *117*, 2937.
- (22) [(**L1Pd**)₂·COD] (**1**) and [(**L2Pd**)₂·COD] were compared as precatalysts for the conversion of an aryl bromide (4-bromovalerophenone) and an aryl triflate (4-pentanyloxyphenyl trifluoromethanesulfonate) to the corresponding aryl fluoride (4-fluorovalerophenone) at room temperature. The reactions were analyzed after 24 h, and these experiments revealed that the use of **1** catalyzes the transformation approximately 3 times faster than the use of [(**L2Pd**)₂·COD] (see the [Supporting Information](#)).
- (23) Huang, S.-M.; et al. *Nature* **2009**, *461*, 614.
- (24) The reduction content (ArH) of **2**, **21**, and **10** was not determined.
- (25) Bissantz, C.; Kuhn, B.; Stahl, M. *J. Med. Chem.* **2010**, *53*, 5061.